

Variable Conductance Heat Pipes: Modelling and Applications

Ad Delil

Abstract

Variable Conductance Heat Pipes (VCHP) differ from other heat pipe types by its thermal control capability: The ability to keep the temperature of a device mounted on the evaporator almost constant, independent of changes of the VCHP boundary conditions (the by the device dissipated power and condenser heat sink).

The only really viable VCHP is of the gas-buffered type. A gas-buffered (or gas-loaded) VCHP can be without or with a cold reservoir (the latter without or with a capillary wick) and with a hot reservoir. Their thermal control properties are limited in case of passive control, even in case of passive feedback control for a VCHP equipped with a bellows reservoir. Perfect temperature control can only be realised using (active) electrical feedback control. A comparison between the various options clearly shows the advantages and drawbacks of the various VCHP options. Aspects of working fluid selection and reservoir sizing will be discussed, including feedback control issues.

The prediction of VCHP control behaviour depends on the particular thermal model used. Mostly this can be done using the Edwards-Marcus flat front model. For some VCHP applications, especially those requiring a VCHP with a low-vapour-pressure working fluid, inertial effects (that can occur for instance during start-up) are to be included in the model. The model developed to account for inertial effects is presented. Modelling outcomes are discussed in detail, including the impact of inertial effects on (active) feedback thermal control.

To conclude, it is illustrated that a Loop Heat Pipe (LHP), which normally operates in the constant conductance mode, is under certain conditions able to operate also in a variable conductance mode.

1. INTRODUCTION

Variable conductance heat pipes (VCHP) are applied in (spacecraft) thermal control to keep the temperature of a heat source as constant as possible for varying thermal loading conditions, i.e. the heat throughput and the temperature of the heat sink. Several methods to achieve VCHP behaviour are described and discussed in literature (Refs. 1 to 7), i.e.:

- Liquid flow control by interrupting or impeding the return of the condensate in the wick. For dissipative heat sources this means just providing "on-off" control, i.e. thermal switching.
- Vapour flow control by interrupting or throttling the vapour flow between the heat pipe evaporator and condenser, which gives rise to the pressure difference, hence the temperature difference, between these regions. The latter means a variable conductance.
- Condenser flooding by non-condensable gas, the so-called gas-loaded VCHP.
- Condenser flooding, being analogous to the gas-loaded concept, but using excess liquid (instead non-condensable gas) to vary the active condenser area.

The best method turned out to be the gas-loading method, i.e. the addition of non-condensable gas to the working fluid. A schematic of such a gas-loaded VCHP is given in figure 1. The gas is swept, by the moving vapour, towards the condenser end. There it forms a gas plug that blocks part of the condenser area for conducting heat to the sink. The size of this plug, in fact a variable conductance, depends on the thermal loading and the pressure in the gas reservoir, usually (but not necessarily) located at the condenser end. This pressure, hence the plug size, can be controlled (for instance in a feedback way) by controlling:

- The temperature of the gas in the reservoir, using a heater (element) and a cooler, e.g. a Peltier element (Fig. 1).
- The gas inventory, using a control valve and an additional gas reservoir.
- The reservoir size, by a bellows system: The so-called variable reservoir volume gas-controlled VCHP (Fig. 2).

The control strongly depends on the transfer function of the VCHP. The performance and the transfer function of a gas-loaded VCHP can be predicted using physical-mathematical models. Though the commonly used Edwards-Marcus model (Ref. 1) is physically incomplete, it will be discussed here to illustrate the working principle, the governing parameters, the sensitivity for parameter variations, etc. The discussions will be restricted to VCHP's with a cylindrical cross-section.

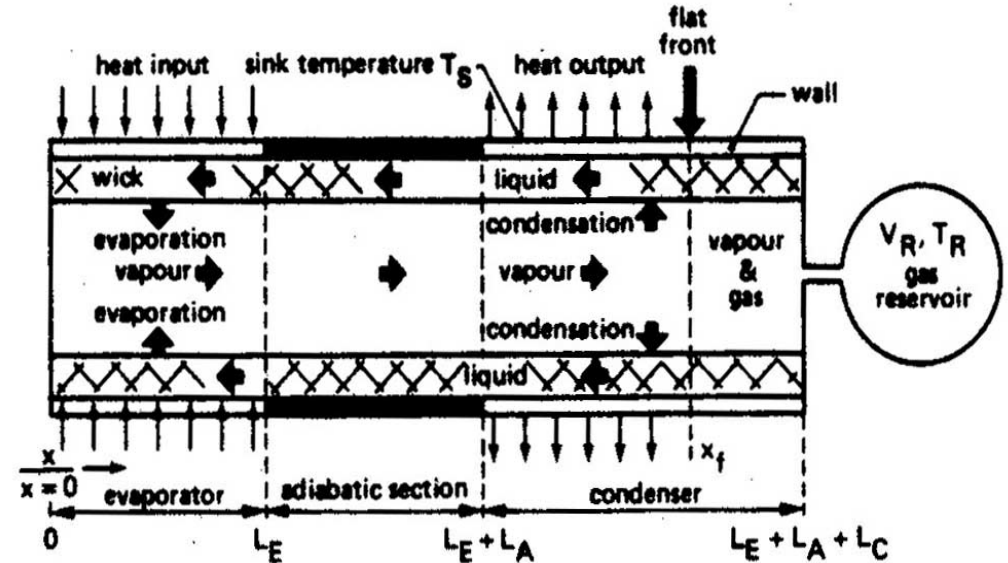


Figure 1. Gas-loaded VCHP, with a wicked or non-wicked reservoir (Ref. 8).

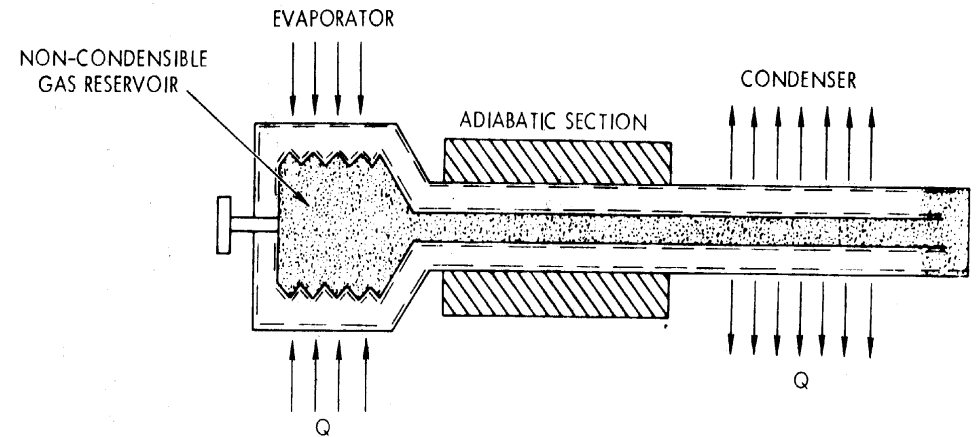


Figure 2. Schematic of a variable reservoir volume gas-loaded VCHP (Ref. 1).

2. THE EDWARDS-MARCUS FLAT FRONT MODEL

Figure 3 schematically depicts a gas-loaded VCHP, and the corresponding temperature distribution according to the Edwards-Marcus flat front model (Ref. 1), which assumes a sharp vapour-gas interface and neglecting axial conduction. In the next sections the approach of reference 1 will be followed more or less before the discussions originally presented in reference 8 will be treated.

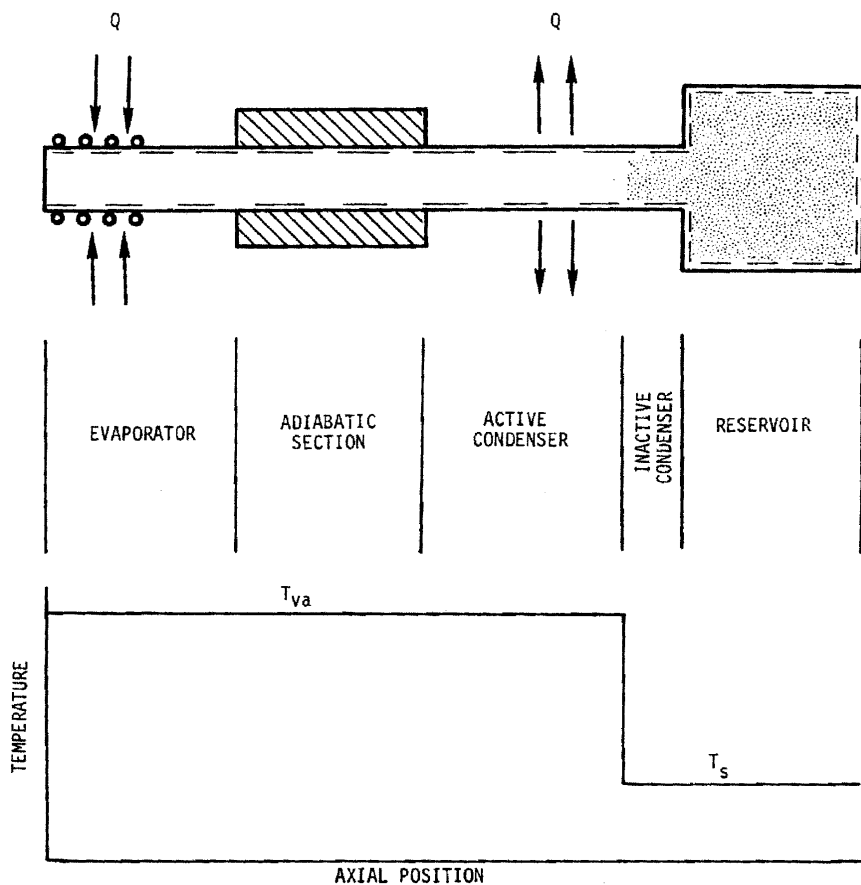


Figure 3. Schematic and flat front temperature distribution of a cold wicked reservoir gas-loaded VCHP (Ref. 1).

Following reference 1, one can write for the equation that describes the simple flat front model for a gas-loaded VCHP without a reservoir ($V_R = 0$):

$$Q = h A' L_a (T_{va} - T_s) \quad (1)$$

Q = transported power, heat load (W); h = heat transfer coefficient (W/m^2K); A' = the heat rejection area per unit

condenser length (m); L_a = active condenser length (m); T_{va} = vapour temperature in the active zone (K), T_s = sink temperature (K).

Assuming that there is no gas in the active part of the heat pipe, the active condenser length L_a can be derived from the requirement that the molar non-condensable gas content n of the VCHP remains constant for all operation conditions, hence:

$$n = p_g (L_C - L_a) A_v / (R_0 T_g) \quad (2)$$

n = total number of gas moles (kmole); p_g = the partial gas pressure (N/m^2); T_g = gas temperature in the pipe volume (K); R_0 = universal gas constant ($8310 J/K \text{ kmole}$), in some figures called R_u ($1.986 \text{ Btu/R lb kmole}$); A_v = cross-sectional area of the vapour core (m^2); L_C = condenser length (m).

For the gas-blocked condenser region one can write

$$T_g = T_s \quad \text{and} \quad p_g = p_{va} - p_{vs} \quad (3)$$

p_{va} = the vapour pressure at T_{va} (N/m^2); p_{vs} = the vapour pressure at T_s (N/m^2).

Combination of (1) to (3) yields

$$Q = h A' (T_{va} - T_s) [L_C - (n R_0 T_s / A_v) / (p_{va} - p_{vs})] \quad (4)$$

Although the above set of equations is somewhat inaccurate, because axial conduction and diffusion effects are being neglected, the errors are quantitative only.

Qualitatively the flat front model allows to do a preliminary design analysis and to identify the major key design parameters, for instance the effect of the working fluid, the effect of variations in sink temperatures, the effect of the working fluid variable sink conditions, wicked and non-wicked reservoir sizing, the control limitations, etc. The term between the brackets represents the active condenser length L_a . Multiplying this by hA' , yields the heat pipe conductance.

2.1. The effect of working fluid for fixed sink conditions

The main goal of a VCHP application is to maintain an almost constant temperature in the active part, in spite of substantially varying heat load and heat sink conditions. Consequently L_a preferably has to be a strong function of the operating temperature T_{va} .

Equation (4) illustrates that, for fixed sink temperature conditions (constant T_s , hence constant p_{vs}), the only fluid parameter that will vary the active condenser length is the operating temperature T_{va} , which sets the corresponding vapour pressure p_{va} . This gives a criterion to properly select the working fluid: Greater control sensitivity can be obtained by using a working fluid that undergoes large vapour pressure changes $\Delta p_{va}/p_{va}$ with temperature, hence large values of $d(\ln p_{va})/dT_{va}$.

In the following considerations, it is assumed that the vapour pressure p_{va} can be approximated by the Clausius-Clapeyron relation, which can be written in differential form, as:

$$d(\ln p_{va})/dT_{va} = (h_{iv} M_v / (R_0 T_{va}^2)) = N_S / T_{va}^2 \quad (5)$$

h_{iv} = latent heat of vaporisation ($J/kmole.K$), in some figures called λ ($Btu/R lbmole$).

N_S is called the gas control sensitivity factor (in K or $^{\circ}R$). It can be used to rank potential working fluids. Figure 4 depicts the temperature dependence of N_S for some candidate working fluids for VCHP applications in space (Note that " T in $^{\circ}F$ minus 32" multiplied by 5/9 yields T in $^{\circ}C$).

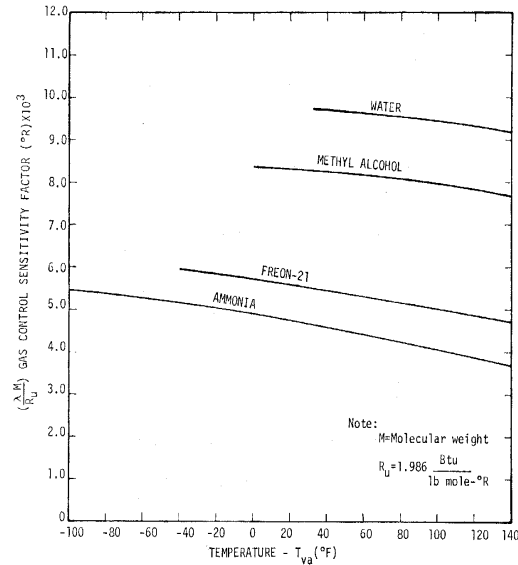


Figure 4. Gas control sensitivity factor versus temperature for some space-related working fluids (Ref. 1).

2.2. The effect of sink temperature variations

The sink temperature T_s influences equation (4) by:

- Altering the maximum heat rejection potential $hA'(T_{va} - T_s) L_{va}$. Consequently, a change in L_{va} is necessary to maintain a given heat transport value.
- Establishing the temperature of the blocked part of the condenser, via the numerator of the second term in brackets. As the volume occupied by the gas also depends on T_s and on the corresponding gas pressure (via the perfect gas law), the gas temperature also influences the gas blocking length.
- Entering the equation as p_{vs} , the vapour pressure of the working fluid at T_s . Within the gas-blocked condenser section, there is always a partial vapour pressure, set by the local temperature. This vapour can be considered as an extra gas inventory, as it has to displace its equivalent in non-condensable gas. This means that, even though there is a fixed inventory of non-condensable gas in the VCHP, the "effective gas contents" is not fixed. It varies with T_s , by controlling the vapour pressure in the region blocked by gas and vapour.

Looking at equation (4) one can see the effect of e.g an increase of T_s :

- Increase of T_s means decrease of $(T_{va} - T_s)$. Consequently the active length has to increase to maintain constant heat rejection Q .
- The increase of the gas temperature leads to an increase of the second term within the brackets. This will lead to a decrease of the active condenser length.
- In addition, an increase of p_{vs} will lead to a decrease of $(p_{va} - p_{vs})$. Consequently the second term within the brackets will increase, and the active condenser length will decrease.

It is evident that the above three effects add up (they do not compensate each other), maximising the increase of T_{va} (and p_{va}) in order to provide the active condenser length increase to maintain the constant heat rejection Q . This is one of the most severe constraints for applying gas-loaded VCHP's.

2.3. The effect of working fluid for variable sink conditions

As it was discussed above: To obtain maximum control sensitivity for fixed sink conditions, a working fluid with a large dp_{va}/dT_{va} at the operating temperature is to be used. But as it was elucidated in the preceding section, the fluid properties enter equation (4) not only as p_{va} , but also as p_{vs} . As variations in p_{vs} adversely affect control, the effect is to be minimised. As p_{vs} enters the equation only as $(p_{va} - p_{vs})$, the absolute variation of p_{vs} (from $T_{s \max}$ to $T_{s \min}$) has to be small as compared to p_{va} . This means that a working fluid with a small p_{vs}/p_{va} -ratio must be selected. It is obvious that a ranking between fluids, based on this criterion, is the same as the ranking of the control sensitivity with fixed sink conditions (Fig. 4), as it is based on a similar criterion. It also can be remarked that there is a problem induced by variable sink conditions when the sink temperature approaches the operating temperature. For applications where the operating temperature is far above the maximum sink temperature, there is no problem at all, since the p_{vs} -term in equation (4) is negligibly small.

2.4. The wicked cold reservoir (for $T_R = T_s$)

Up to now the gas was contained in the non-active condenser region ($V_R = 0$). But as said before: To realise high control sensitivity, the active condenser length L_a shall be a strong function of the operating pressure p_{va} . This means that L_a has to be a strong function of the operating pressure p_{va} . As the moving of the vapour-gas front implies compression of the gas inventory, one must minimise the relative gas compression $\Delta V_g/V_g$ needed to move the front. This usually is realised by adding a gas reservoir with a large volume ($V_R \gg A'L_C$) outside of the region of the vapour-gas front travel (Figs. 1 to 3). The gas can flow in and out this reservoir.

Figure 3 also depicts the flat front temperature distribution for the very realistic case of a VCHP with a cold internally wicked reservoir that can be assumed to be in thermal equilibrium with the same environment as the gas-blocked condenser section ($T_g = T_R = T_s$). Since the molar gas inventory pertains now to both the inactive condenser part and the reservoir, a reservoir term has to be added to the molar gas equation (2), yielding

$$n = p_g [(L_C - L_a) A_v + V_R] / (R_0 T_g), \quad (6)$$

and transferring equation (4) into

$$Q = h A' (T_{va} - T_s) [L_C + (V_R/A_v) - (n R_0 T_s/A_v) / (p_{va} - p_{vs})], \quad (7)$$

the term in brackets represents the active length.

For a given sink temperature, the VCHP control range corresponds to the active length range: 0 to L_C . The latter corresponds to maximum heat transport

$$Q_{\max} = hA (T_{va \max} - T_s) L_C. \quad (8)$$

Normalising equation (7), using equation (8) and inserting $L_C A_v = V_C$ yields the general equation for the control sensitivity of a cold wicked reservoir VCHP:

$$(T_{va} - T_s)/(T_{va \max} - T_s) = (Q/Q_{\max}) (V_C/V_R) / [1 + (V_C/V_R) - (n R_0 T_s/V_R) / (p_{va} - p_{vs})], \quad (9)$$

being independent of external geometry A' and heat transfer coefficient h , and clearly illustrating the effect of the reservoir volume V_R , entering the equation via n/V_R and V_C/V_R . The term n/V_R determines the maximum set-point temperature $T_{va \max}$ for a given sink temperature T_s .

The term V_C/V_R determines the control sensitivity: Equation (9) clearly shows that for large reservoirs ($V_R/V_C \gg 1$) the term in brackets becomes a stronger function of p_{va} , hence the control sensitivity increases, meaning a decrease of the variation in T_{va} with Q . This is quantitatively illustrated by figure 5, depicting a typical example for a space-related VCHP application.

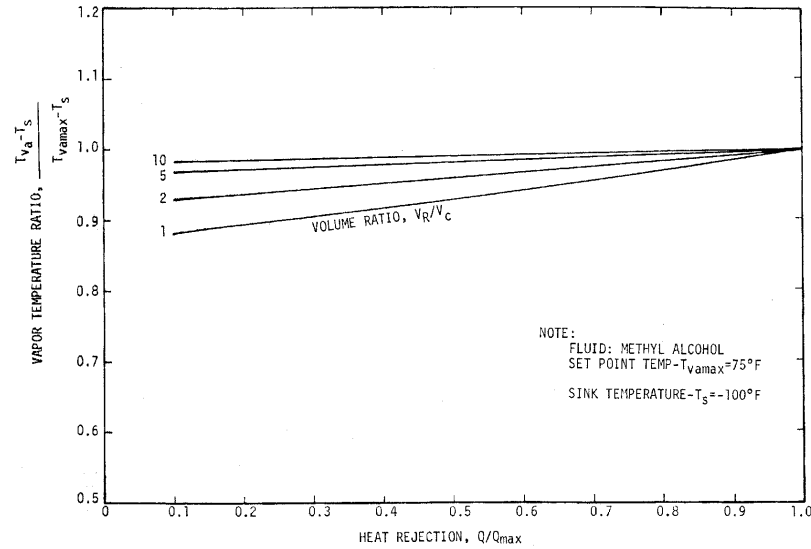


Figure 5. Effect of V_R/V_C on control sensitivity for methanol: $T_R = T_s$; set-point $T_{va\ max} = 38^\circ\text{C}$, sink $T_s = 22^\circ\text{C}$ (Ref. 1).

2.5. The wicked cold reservoir (for $T_R \neq T_s$)

As discussed earlier (for $V_R = 0$), severe control constraints originate from variations in environmental conditions: Changes in gas temperature and the partial vapour pressure in the gas-blocked region. Adding a reservoir, an extension of the blocked zone, amplifies this effect, like it amplifies control sensitivity. Consequently, for VCHP applications with large excursions of sink conditions one has to control the reservoir such that its temperature fluctuates less, being a reservoir which is not in thermal equilibrium with the same environment as the gas-blocked condenser section ($T_R \neq T_s$). For this more general case (for which $T_g = T_s$ and $p_g = p_{va} - p_{vs}$ for the blocked condenser region, and $T_g = T_R$ and $p_g = p_{va} - p_{vR}$ for the condenser), one can derive like done before for the $T_R = T_s$ case:

$$n = (p_{va} - p_{vs}) (L_C - L_a) A_v / (R_0 T_s) + (p_{va} - p_{vR}) V_R / (R_0 T_R) \quad (10)$$

$$L_a = L_C - [(R_0 T_s) / (p_{va} - p_{vs})] [n - (p_{va} - p_{vR}) V_R / (R_0 T_R)] \quad (11)$$

$$Q = h A' (T_{va} - T_s) [L_C + (V_R/A_v) (T_s/T_R) (p_{va} - p_{vR}) / (p_{va} - p_{vs}) - (n R_0 T_s/A_v) / (p_{va} - p_{vs})]. \quad (12)$$

A comparison between the equations (12) and (7) clearly shows that the effect of non-equilibrium ($T_R \neq T_s$) is the multiplication of the V_R/A_v -term by $(T_s/T_R) (p_{va} - p_{vR}) / (p_{va} - p_{vs})$. The latter reduces of course to unity for $T_R = T_s$.

In the preceding section, it was shown that the control sensitivity improves with increasing V_R/V_C . As for a given condenser length L_C , V_R/V_C is proportional to V_R/A_v , it is clear that the second term within the brackets represents the impact of the reservoir: For maximum control sensitivity, this term is to be maximised.

As the term $(T_s/T_R) (p_{va} - p_{vR}) / (p_{va} - p_{vs})$ is < 1 for $T_R > T_s$, equal to 1 for $T_R = T_s$, and > 1 for $T_R < T_s$, it is clear that for a given condenser sink temperature T_s and reservoir size V_R , the control sensitivity $\partial Q/\partial T_{va}$ will increase for $T_R < T_s$ and decrease for $T_R > T_s$.

But the principal objective of thermally de-coupling of the reservoir from the condenser sink ($T_R \neq T_s$) is to minimise the impact of condenser sink temperature variations, and is not the control sensitivity issue. Equation (12) clearly shows this: Variations in T_s proportionally effect the second and third terms, for fixed T_R (hence V_R). The effects of the two terms (partly) compensate each other, as they have opposite signs. For equal (varying) values of $T_R = T_s$, this compensation disappears.

Keeping the reservoir temperature (T_R) constant implies a decrease of the VCHP sensitivity for variations in sink (T_s) conditions. Preferably one wants even to keep T_R constant at a value below T_s to increase the control sensitivity $\partial Q/\partial T_{va}$. Unfortunately this is often not possible for spacecraft-related VCHP applications, since the condenser heat rejection usually is via a radiator, radiating to cold space and a reservoir environment below the effective (radiating) sink temperature is simply not available.

2.6. The non-wicked reservoir

As said before, the most effective approach to minimise the effects of sink temperature fluctuations is by controlling the wicked reservoir temperature. Unfortunately for space-related applications this will usually require thermostatically controlled heaters on the reservoir, which means the loss of the major advantage of the simple gas-loaded VCHP, namely passive operation. Additional disadvantages are the need of power and the inherent reduction of system reliability.

Figure 6 depicts the non-wicked reservoir solution, a compromise, which still yields a passive system.

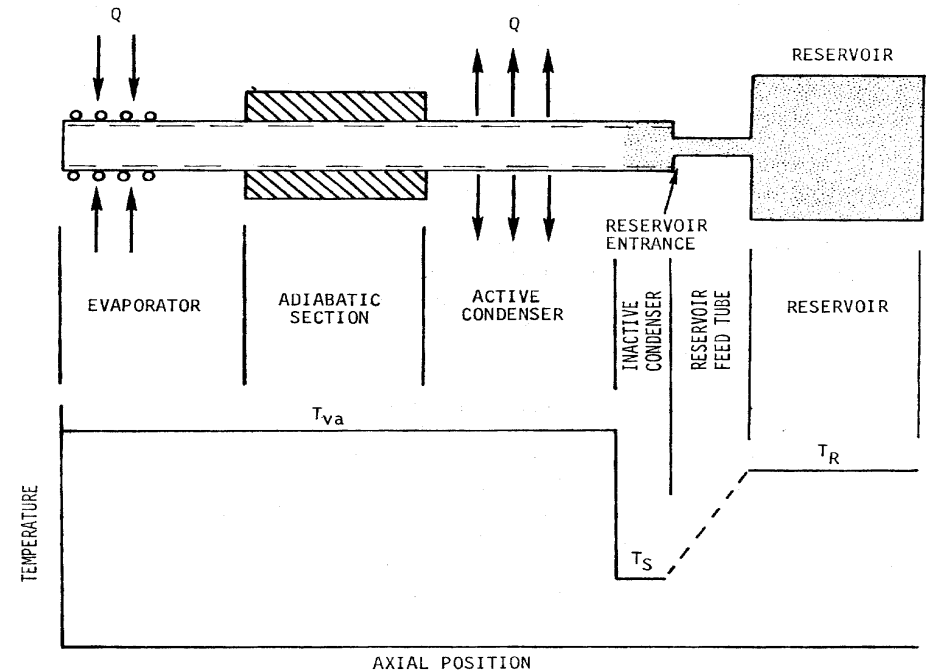


Figure 6. Schematic and flat front temperature distribution of a hot non-wicked reservoir gas-loaded VCHP (Ref. 1).

The effect of removing the wick simply is to replace in equation (12) p_{vR} by p_{vs} , yielding:

$$Q = h A' (T_{va} - T_s) [L_C + (V_R/A_v) (T_s/T_R) - (n R_0 T_s/A_v) / (p_{va} - p_{vs})]. \quad (13)$$

Like for a controlled temperature wicked reservoir system, control of the temperature of a non-wicked reservoir minimises the impact of sink temperature variations on the gas temperature. But, unlike the controlled temperature wicked reservoir system, the non-wicked reservoir system is suffering from partial vapour pressure variations inside the reservoir (p_{vs}) with variations of T_s . In other words, it is less sensitive for T_s -variations than an uncontrolled wicked reservoir VCHP (where $T_R = T_s$), but more sensitive for T_s -variations than the controlled temperature wicked reservoir VCHP, with fixed T_R . For detailed discussions on this issue and on the effects of thermal diffusion, it is referred to the references 1, 9 and 10. A disadvantage of the non-wicked system is that mass diffusion (a slow process) might impair the transient response characteristics of the VCHP (Refs. 1, 4).

A major advantage of the non-wicked over the wicked reservoir system is the fact that the reservoir temperature T_R needs not to be much lower than the evaporator temperature T_{va} . T_R can be equal or even higher than T_{va} . This offers a simple possibility to provide close reservoir temperature control (independent of the thermal environment and without the use of heaters and thermostats), by thermally coupling the reservoir directly to the evaporator, either in contact with it, or in it (Fig. 7).

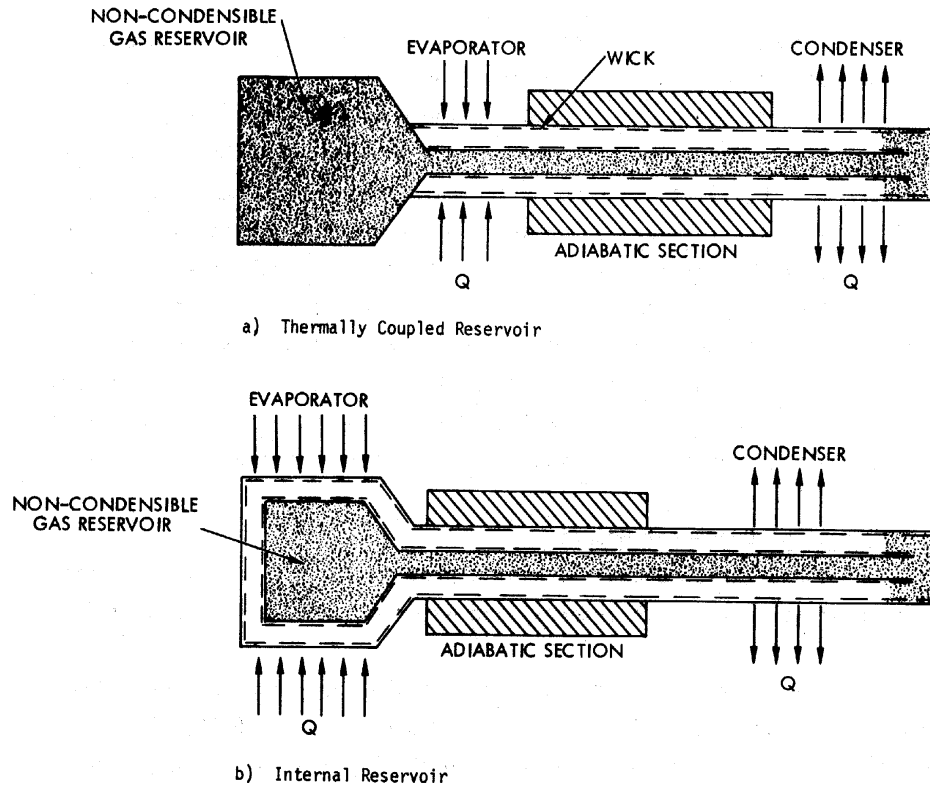


Figure 7. Schematic diagrams of hot non-wicked reservoir VCHP's: (a) Thermally coupled and (b).Internal (Ref. 1)

2.7. Reservoir sizing

As discussed in detail in reference 1, the reservoir sizing procedure consists of writing down the characteristic equation for the two extreme operating cases, the fully open condenser at maximum thermal boundary conditions and the fully closed condenser at minimum thermal boundary conditions. This has to be done without specifying the reservoir volume and gas inventory. The obtained equations are to be simultaneously solved for the reservoir volume and the molar gas inventory, while the other parameters are to be specified.

The procedure will be elucidated for the special case of a wicked reservoir with $T_R = T_s$, under the assumption that the extremes in heat rejection, $Q_{max} = h A' (T_{va max} - T_{s max}) L_C$, respectively $Q_{min} = 0$, correspond to the extremes in active condenser length $L_{max} = L_C$, resp. $L_{min} = 0$. This yields the following two equations

$$Q = h A' (T_{va max} - T_{s max}) [L_C + (V_R/A_v) - (n R_0 T_{s max}/A_v) / (p_{va max} - p_{vs max})] = h A' (T_{va max} - T_{s max}) L_C, \quad (14a)$$

$$Q = h A' (T_{va min} - T_{s min}) [L_C + (V_R/A_v) - (n R_0 T_{s min}/A_v) / (p_{va min} - p_{vs min})] = 0, \quad (14b)$$

which can be written as

$$V_R/A_v = (n R_0) (T_{s max}/A_v) / (p_{va max} - p_{vs max}) \quad \text{and} \quad L_C + V_R/A_v = (n R_0) (T_{s min}/A_v) / (p_{va min} - p_{vs min}). \quad (15a,b)$$

Elimination of $(n R_0)$ in (15a,b) yields

$$n R_0 = (V_R/A_v) A_v (p_{va max} - p_{vs max}) / T_{s max} = (L_C + V_R/A_v) A_v (p_{va min} - p_{vs min}) / T_{s min}, \quad (16)$$

or after inserting $V_C = L_C A$, the simple expression for condenser to reservoir volume ratio

$$V_R/V_C = 1 / [\{ (T_{s min}/T_{s max}) (p_{va max} - p_{vs max}) / (p_{va min} - p_{vs min}) \} - 1]. \quad (17)$$

Equation (17) was derived for the special case of a wicked reservoir with $T_R = T_s$ and $0 \leq L_a \leq L_C$.

Similar exercises for other cases yield similar results, though the algebra is somewhat more cumbersome. For the general wicked reservoir case (with $T_R \neq T_s$, $Q_{min} \neq 0$ and $L_a \neq L_C$ at Q_{max} , $T_{s max}$ and $T_{s min}$) one can derive:

$$V_R/V_C = (\xi_1 - \xi_2) / \xi_3, \quad (18)$$

$$\xi_1 = [(p_{va min} - p_{vs min}) / T_{s min}] [1 - Q_{min} / \{L_C h A' (T_{va min} - T_{s min})\}], \quad (18)$$

$$\xi_2 = [(p_{va max} - p_{vs max}) / T_{s max}] [1 - Q_{max} / \{L_C h A' (T_{va max} - T_{s max})\}], \quad (18)$$

$$\xi_3 = [(p_{va max} - p_{vR max}) / T_{R max}] - [(p_{va min} - p_{vR min}) / T_{R min}]. \quad (18)$$

A modified version of the equations (18) yields the generalised equation for a non-wicked reservoir VCHP, by substituting $p_{vs max}$ for $p_{vR max}$ and $p_{vs min}$ for $p_{vR min}$. For the special case where the reservoir is coupled to the evaporator ($T_R = T_{va}$) and $0 \leq L_a \leq L_C$ for $0 = Q_{min} \leq Q \leq Q_{max} = L_C h A' (T_{va max} - T_{s max})$ one can derive the equivalent of (17):

$$V_R/V_C = 1 / [\{ (T_{s min}/T_{va max}) (p_{va max} - p_{vs max}) / (p_{va min} - p_{vs min}) \} - (T_{s min}/T_{va min})]. \quad (19)$$

The equations (17) and (19) are very useful, as they yield the required reservoir to condenser volume ratios, as a function of the anticipated variations in sink temperature and the specified control range. Although they are special cases of the generalised equation (18), they are very realistic since:

- Hot non-wicked reservoirs will often be coupled to the evaporator (a stable temperature region).
- Cold wicked reservoirs will often see the same environment as the condenser ($0 \leq L_a \leq L_C$ for $0 = Q_{min} \leq Q \leq Q_{max}$).
- The assumption of a fully utilised condenser is a realistic design goal.

In conclusion it can be said that the equations yield a simple, straightforward method for a parametric analyses on how the choice of the working fluid, expected sink conditions and control range specifications have their impact on the reservoir sizing. They also yield a practical basis for the comparison of hot non-wicked and cold wicked designs. The procedures that led to the equations can also provide expressions for any gas-loaded VCHP configuration, including wicked or non-wicked reservoirs, controlled or floating temperature reservoirs, multi-section condensers, such as cold traps, gas-blocked adiabatic sections, etc. (Ref. 1).

As an example, figure 8 illustrates the above by presenting the results of calculations for a typical spacecraft control application. The equations (17) and (19) were to be solved for reservoir sizing, requiring T_{va} to be $21\text{ }^{\circ}\text{C}$ ($70\text{ }^{\circ}\text{F}$) $\pm T_{va}/2$ and an anticipated sink temperature, varying between $-104\text{ }^{\circ}\text{C}$ ($-156\text{ }^{\circ}\text{F}$) and $-42\text{ }^{\circ}\text{C}$ ($-44\text{ }^{\circ}\text{F}$). The curves illustrate the required V_R/V_C to realise the specified control range for methanol-filled VCHP's, one with a hot non-wicked, the other with a cold wicked reservoir, and an ammonia-filled VCHP, with a hot non-wicked reservoir.

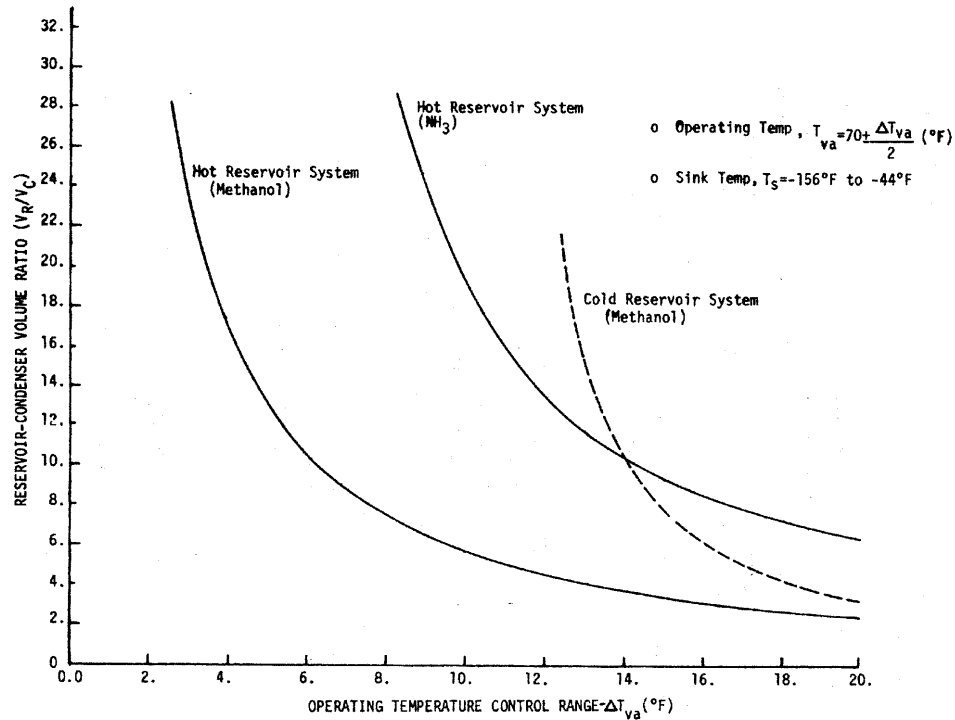


Figure 8. Reservoir volume requirements versus temperature control range (Ref. 1).

The figure clearly shows that:

- Methanol offers a much closer control than ammonia for the hot reservoir system. This is also true for the cold reservoir systems, as it basically reflects the fluid vapour pressure characteristics discussed.
- The hot non-wicked reservoir option offers much closer control than the cold wicked reservoir option. This holds for passively controlled heat pipes, regardless of the working fluid used.

The quantitative curves of figure 8 are not general, but the qualitative conclusions are generally correct.

The effects of sink temperature variations were already qualitatively discussed. Quantitative information can be seen in figure 9, showing the hot and cold reservoir sizing for different typical spacecraft effective sink temperatures. The fluid is methanol, the nominal set-point is $21\text{ }^{\circ}\text{C}$ ($70\text{ }^{\circ}\text{F}$). The figure confirms that the hot non-wicked reservoir option offers much closer control than the cold wicked reservoir option. But it is also shown that the hot non-wicked reservoir system is much less sensitive to sink temperature variations.

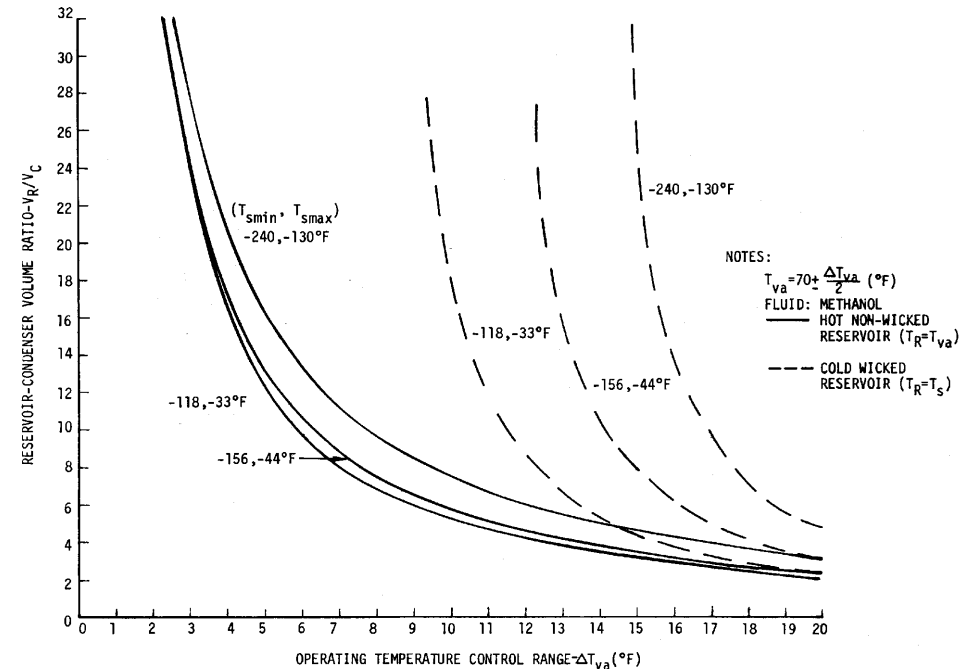


Figure 9. Reservoir volume requirements versus temperature control range (Ref. 1).

2.8. Limitations of passive control

The figures 8 and 9 show an important fact regarding the passive temperature control limits: Variations of the effective sink temperature set the lower control limit, regardless of how large the reservoir is. It is obvious, according to equation (6), that temperature control for fixed sink conditions is perfect for V_R/V_C -ratios approaching infinity. But the two figures indicate that the control band ΔT_{va} approaches finite positive limits for varying sink conditions, if V_R/V_C approaches infinity. The magnitudes of these limits depend on the working fluid, the nominal operating temperature T_{va} and the particular sink temperature range involved.

2.9. The variable set-point VCHP

A viable approach to obtain a variable set-point is by keeping the gas inventory constant and varying the reservoir volume, e.g. via an internal bellows system (Fig. 2). An external bellows system is also possible, but in that case there will be a pressure difference across the reservoir wall, which varies with internal or external pressure variations. This can be cured only at the cost of a considerable increase of system complexity. When the bellows reservoir is inside the heat pipe, the total pressure within it is equal to the pressure surrounding it. Consequently the problem is eliminated.

The characteristic equation for the internal non-wicked reservoir system follows from equation (13) by replacing p_{vR} by p_{vs} , yielding:

$$Q = h A' (T_{va} - T_s) [L_C + (V_R/A_v) (T_s/T_{va}) - (n R_0 T_s/A_v) / (p_{va} - p_{vs})]. \quad (20)$$

This equation shows that a change in V_R causes a change in T_{va} . But this is not an identical approach as changing the gas inventory (which is not practical as it requires very complex metering devices to precisely control the gas and working fluid inventories). Varying the bellows volume changes both the control sensitivity and the set-point. This is shown in figure 10, depicting for constant T_s , the dependence of T_{va} on heat load Q for variable and fixed internal reservoir systems.

The curves show that increasing the set-point temperature, by increasing the molar inventory n or decreasing the reservoir volume V_R , leads to a substantially degraded variable volume VCHP as compared to the variable inventory VCHP. This means that the variable volume VCHP is considerably simpler than the fixed volume variable inventory alternative, it has far lower control sensitivity, especially at high operating temperatures.

For the alternative set-point control solution, being the already discussed reservoir temperature control, there are two different operational modes: One for a non-wicked reservoir option, the other for the wicked reservoir option. This issue is discussed in detail in reference 1.

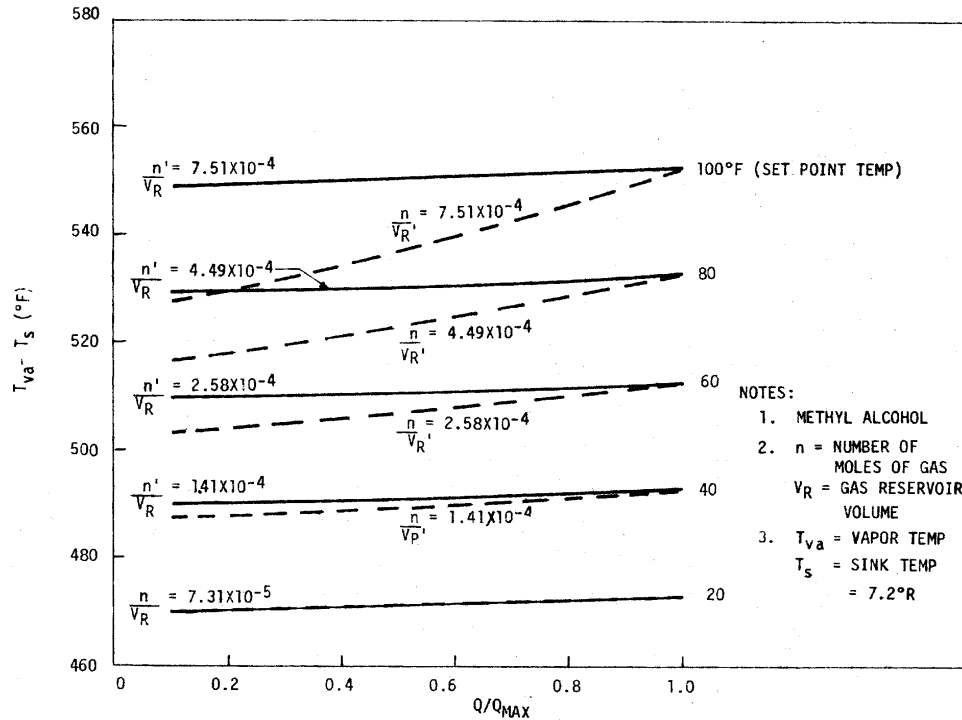


Figure 10. Comparison of gas inventory versus reservoir volume (Ref. 1).

2.10. The Feedback controlled VCHP

A feedback controlled VCHP essentially is a VCHP that includes an external feedback control loop. The most attractive controls the wicked reservoir via an electronic or thermostatic control circuit, that maintains the heat source at the specified temperature by the power fed to the reservoir heater or cooler (Peltier element). Such a system is schematically depicted in figure 11.

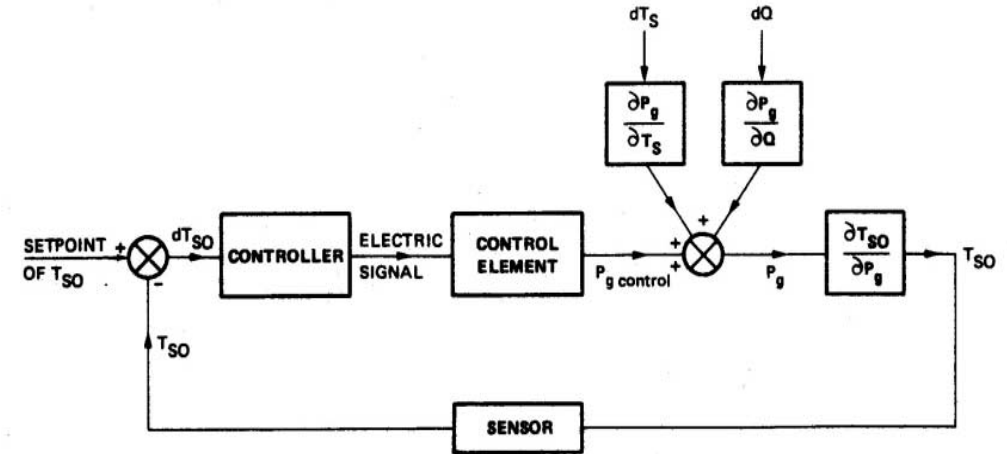


Figure 11. Feedback controlled gas-loaded heat pipe (Ref. 8)

The behaviour of a feedback controlled VCHP (or FCHP), fundamentally being a wicked reservoir heat pipe with $T_R \neq T_s$, is described by equation (12), in which T_R is a non-fixed parameter (which complicates the parametric design procedure. It is remarked that:

- Like for a passively controlled VCHP, the FCHP control implies that the maximum reservoir temperature must be equal or lower than the evaporator temperature, to prevent that the reservoir becomes the evaporator.
- Unlike it is the case in a passively controlled VCHP, where $\partial T_{va}/\partial Q$ is always positive (and approaches zero for $V_C/V_R \rightarrow \infty$), the FCHP allows to lower the evaporator temperature for increasing heat input, meaning negative $\partial T_{va}/\partial Q$. Consequently the actively controlled FCHP yields a closer temperature control of the heat source than a passive system does.
- Unlike for a passively controlled VCHP, the better control in an FCHP will be realised by the use of working fluids with a high value of p_{vR}/p_{va} because T_R decreases from T_{va} . In other words, where methanol is superior to ammonia in passive systems, ammonia is superior to methanol in the heated wicked reservoir FCHP.
- Further information on the steady-state and transient performance of FCHP can be found in the references 5 to 7.

3. THE NLR IMPROVED MODEL FOR GAS-LOADED VCHP

Recalling figure 1 and the earlier made statement that the commonly used model is incomplete. Therefore NLR developed a transient model (Refs. 8 to 13), intended that it can be easily implemented in existing general thermal analyzer computer programs. The model developed so far is steady-state. It accounts for the following effects: diffusion at the vapour-gas interface, radial thermal conduction in the wall and wick of the heat pipe and friction and inertia in the moving vapour.

Calculations have been carried out for a parameter analysis that clearly showed that the effect of diffusion is negligible as compared with the frictional and inertial effects (Refs. 9, 10). This consequently led to the current flat front model being the aforementioned uniaxial model in its limit of zero diffusivity (Ref. 9). Using this model it has been shown that inertial effects can be considerable in that part of the heat pipe operating range that is characterised by low vapour pressures. This turns out to be a rather wide range for heat pipe working fluids with relatively low vapour pressures, such as methanol, ethanol and the liquid metals (Ref. 8, 11, 13). For other working fluids this range is only a narrow one, close to the freezing point. Since the net effect of friction is increasing the velocity of a subsonic flow, friction enhances the impact of inertial effects and it widens the above-mentioned operating range (Refs. 8 to 13). Friction also lowers the sonic limitation to the heat transport capability making a heat pipe more sensitive for blocking of the heat transport by choking (Refs. 8 to 13).

In the condenser section inertia decelerates the vapour flow leading to temperature and pressure increase. Friction counteracts this by accelerating the vapour flow. Usually the effects of inertia dominate frictional effects. However, operating conditions have been identified where frictional effects are dominant, especially for front positions far from the condenser entrance. In these situations small variations in thermal loading yield very large front displacements, accompanied by transfer functions unfavourable for (feedback) control systems.

Calculations have been performed with the computer program based on the current model. The results of these calculations are used:

- To design a VCHP for the experimental verification of the model developed.
- To define test schemes and proper test conditions to predict VCRP transfer functions for control purposes.
- To identify possible problem areas, especially with respect to limitations in performance and control.

Since the aforementioned calculations are straightforward and easy to perform, implementation of the NLR model in existing thermal analyzer programs for spacecraft is considered to be simple. This implementation will be realised after completing the model with axial conduction. It is also expected that the complete model constitutes an adequate basis for modelling the transient behaviour of a gas-loaded VCHP at reasonable costs.

3.1. Assumptions and restrictions

The following restrictions and assumptions are made:

- The model is uniaxial and applicable to cylindrical VCHP's only, in other words for VCHP's with homogeneous or axially grooved wicks (to transport the condensed working fluid back to the evaporator). More complicated wicks are of the arterial or pedestal type. Also, different locations of the vapour passage or gas reservoir occur. Though vastly different in construction details there is no difference with respect to the modelling of phenomena in the vapour passage of VCHP's. Therefore, results obtained for the simple cylindrical configuration contribute to understand the performance of more complicated configurations.
- Only steady-state conditions are considered.
- Axial heat conduction by the wall and wick is not taken into account.
- The radial heat transfer per unit of condenser (evaporator) area is proportional to the difference between the vapour temperature and the sink (source) temperature. This means that the radial conduction properties do not depend on the temperature. This is a good approximation for not too large temperature intervals.
- Diffusion is set zero, since its effects have been shown to be negligible compared with inertial effects (Refs. 9, 10).
- The vapour has a constant viscosity and obeys the Clausius-Clapeyron relation.

$$\rho_v = \alpha M_v / (R_0 T) \exp(-N_S / T), \quad (21)$$

α is a reference pressure (proportionality constant). N_S is a control sensitivity factor, being:

$$N_S = (h_{iv} M_v / (R_0)). \quad (22)$$

This is justified for not too large temperature intervals since for most working fluids and h_{iv} show only little variation within a large temperature interval at the freezing point side of the operating range.

3.2 The model equations

The governing flat front equations can be written as (Ref. 13, 8):

$$\begin{pmatrix} \frac{\rho_v}{M_v} & u & 0 \\ \beta \rho_v u & R_0 T & \frac{R_0 \rho_v}{M_v} \\ 0 & \frac{M_v}{\rho_v} & -\frac{N_S}{T^2} + \frac{1}{T} \end{pmatrix} \begin{pmatrix} \frac{du}{dx} \\ \frac{1}{M_v} \frac{d\rho_v}{dx} \\ \frac{dT}{dx} \end{pmatrix} = \begin{pmatrix} -\frac{Q_i}{A_c h_{lv} M_v} \\ -\frac{2f \rho_v u^2}{d} + \frac{u Q_i}{A_c h_{lv}} (\beta - f) \\ 0 \end{pmatrix} \quad (23)$$

being the constitutive equations for compressible fluid flow integrated over the cross-sectional area (Ref. 14), and the differential form of the Clausius-Clapeyron relation. Q_i (or Q) is the heat input. β is the shape (flow profile) factor for the velocity profile, varies from 1 for pure plug flow to 4/3 for pure laminar flow. f is a friction factor that can be approximated (Refs. 12, 14, 15) by:

$$f = 16/Re \quad \text{for laminar flow (Re} < 2000), \quad (24)$$

$$f = 0.079/(Re)^{1/4} \quad \text{for turbulent flow (Re} > 2000). \quad (25)$$

$$Re = \rho_v u d / \mu_v \quad (26)$$

is the Reynolds number.

The hydraulic diameter d equals 4 times the ratio between cross-sectional area and perimeter. A discussion on the friction factor f for heat pipes is presented in reference 15, in which friction factors up to 3 times the smooth pipe values are calculated possible.

γ accounts for the transition of radial to axial momentum. It is assumed to be negligible for $Re < 2000$, and is for $Re > 2000$ approximated by

$$\gamma = 1 - 2000/Re. \quad (27)$$

Further it is specified for the heat input per unit length Q_i that:

$$Q_i = B (T_{SO} - T) \quad \text{in the evaporator } 0 \leq x \leq L_E, \quad (28a)$$

$$Q_i = 0 \quad \text{in the adiabatic section } L_E \leq x \leq L_E + L_A, \quad (28b)$$

$$Q_i = A(T - T_S) \quad \text{in the condenser } L_E + L_A \leq x \leq L_E + L_A + L_C. \quad (28c)$$

The total heat throughput can be obtained by integrating Q_i

$$Q = \int_{L_E + L_A}^{L_E + L_A + L_C} A(T - T_S) dx = \int_0^{L_E} B (T_{SO} - T) dx. \quad (29)$$

Additional relations are the equations of state for the vapour and for the control gas:

$$P_v = (\rho_v / M_v) R_0 T_v, \quad (30)$$

$$P_g = (\rho_g / M_g) R_0 T_g. \quad (31)$$

Finally it is remarked that $u = 0$ at the flat front position x_f where the temperature is discontinuous i.e. equal to T_f at the upstream side and T_S at the downstream side. The pressure is continuous in the entire VCHP. Pressure equilibrium yields the gas control relation

$$p_g = (\rho_g/M_g) R_0 T_S = \alpha [\exp(-N_S/T_i) - \exp(-N_S/T_S)], \quad (32)$$

and the molar gas content

$$n_g/M_g = (\alpha A_C/R_0 T_S) (L_E + L_A + L_C - x) [\exp(-N_S/T_i) - \exp(-N_S/T_S)] + (\alpha V_R/R_0 T_R) [\exp(-N_S/T_i) - \exp(-N_S/T_S)] \quad (33)$$

Equation (3) becomes singular if and only if the determinant of the 3x3 matrix is zero. This is equivalent with a critical velocity

$$u_s = [\{ N_S/(N_S - T) \} \{ R_0 T/(\beta M_v) \}]^{1/2}, \quad (34)$$

being the velocity of sound $(\partial p_v/\partial \rho_v)^{1/2}$, as it straightforwardly follows from the equations (30) and (21).

The corresponding sonic limit of the heat throughput is:

$$Q_s = \rho_v A_C h_{iv} u_s = [\{ N_S/(N_S - T) \} \{ R_0 T/(\beta M_v) \}]^{1/2} (\alpha A_C N_S) \exp(-N_S/T). \quad (35)$$

4. QUANTITATIVE CONSIDERATIONS

Various calculations have been carried out in order to define a test heat pipe and test conditions for the experimental verification of the model. A correct definition of the VCHP and the test conditions will yield detectable frictional and inertial effects. In addition requirements for easy experimenting, preferably not too far from room temperature, must be met. Based on these requirements and on the results of the calculations a "SABCA M96-like VCHP has been selected (Ref. 8). The working fluid is methanol: The fluid properties are listed in the references 2, 15 to 18. Characteristics of the heat pipe are: external diameter 9.5 mm, (stainless steel) wall thickness 0.5 mm, composite wick consisting of one circumferential mesh layer and a centrally located 8-shaped mesh filled artery (yielding a vapour core cross sectional area of $2.6 \cdot 10^{-5} \text{ m}^2$ and a hydraulic diameter of 2.03 mm). The evaporator length, being no characteristic, is chosen to be 0.1 m. Results of calculations performed for this selected heat pipe are discussed in the sequel.

4.1. Temperature and velocity distributions

Figure 12 shows an example of calculated temperature and vapour velocity distributions along the pipe. The figure clearly illustrates the accelerating effect of friction, which especially at higher throughput values leads to performances (front positions, front temperatures) which considerably differ from the corresponding zero-friction performances. This consequently leads to differences in transfer functions. The figure also illustrates that in the condenser friction becomes dominant at the highest throughput values only. For lower throughput inertia dominates friction (temperature and pressure recovery).

Finally it is remarked that the accelerating effect of friction is accompanied by a decreasing of the vapour temperature. This limits the maximum throughput for given source and sink conditions, since the vapour temperature at the condenser entrance must be higher than the sink temperature.

4.2. Choking

Choking (Refs. 14, 15, 18, 19), occurring when the local vapour velocity becomes equal to the velocity of sound, limits the heat throughput of a heat pipe. In models neglecting friction choking adjusts the maximum throughput for conditions pertaining to the evaporator exit, where the vapour flow reaches its maximum velocity and the velocity of sound its minimum value. When friction is taken into account choking can take place in every heat pipe section, depending on the various thermal loading conditions. This is illustrated in figure 13. In all cases, however, friction lowers the sonic limitation to the heat throughput.

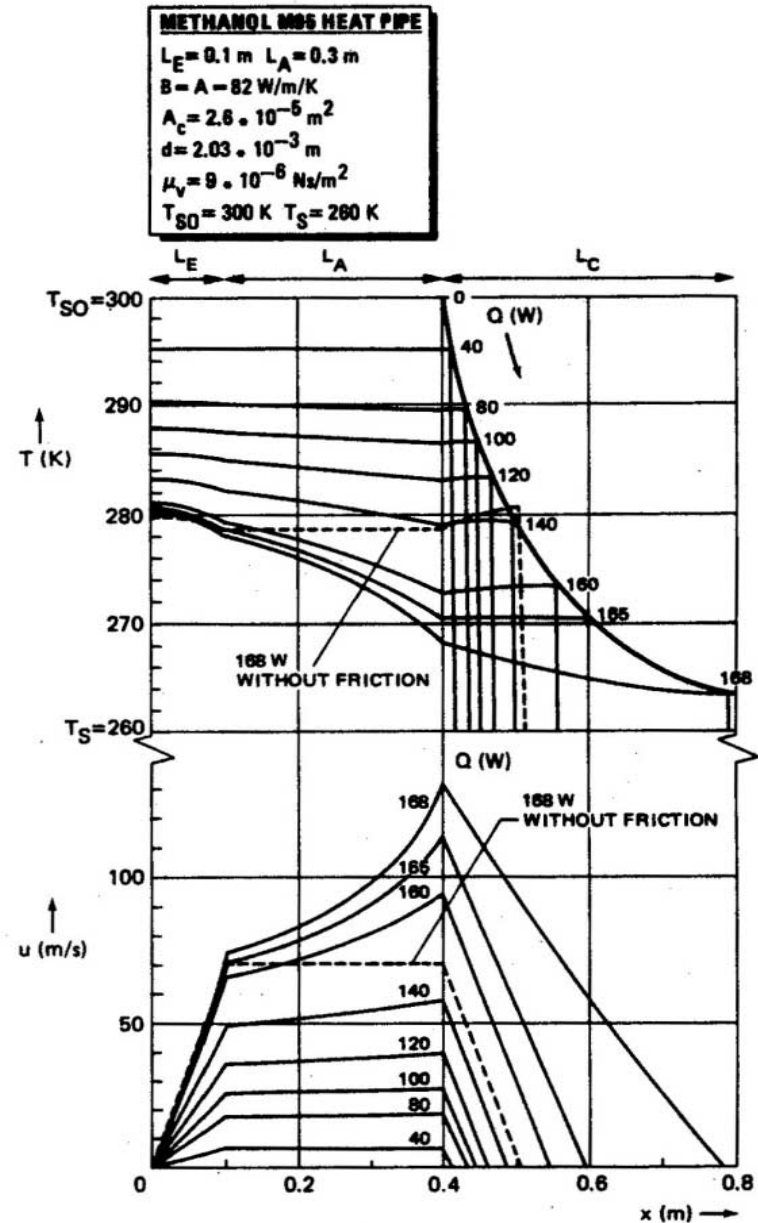


Figure 12. Vapour velocity and temperature distribution in the methanol M95 heat pipe for various heat throughputs (Ref. 8).

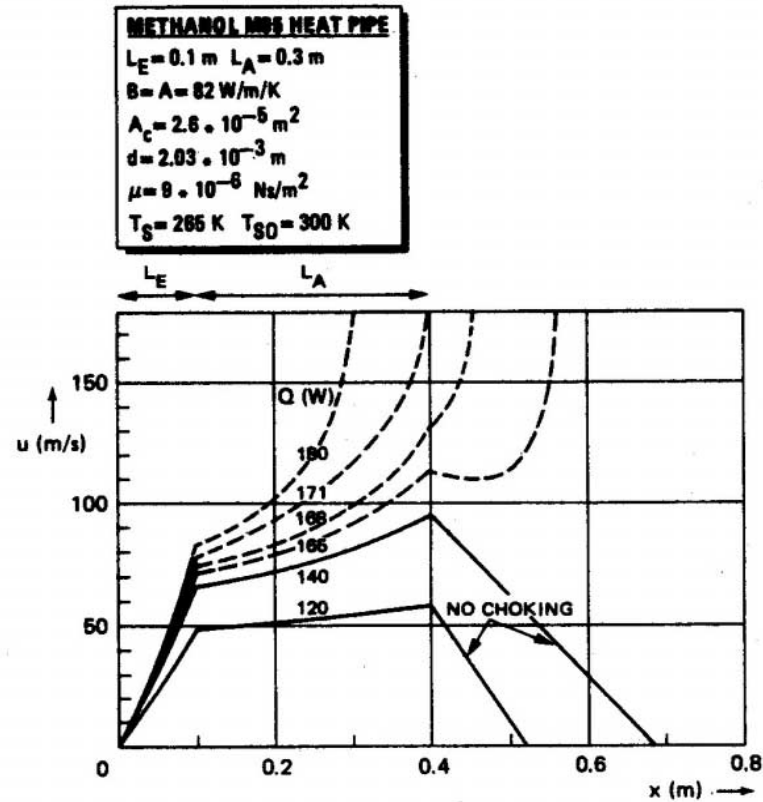


Figure 13. Choking, for increasing throughput shifting from condenser to adiabatic section (Ref. 8).

4.3. Maximum throughput figures

Iterative calculations with the computer program developed yield the figures 14 to 18, quantifying the substantial maximum throughput reduction caused by friction.

From figure 14, illustrating the influence of the flow profile factor S , it can be concluded that - for the heat pipe selected - the outcomes hardly depend on S if friction is taken into account. Since at the low pressure side of the operating range Reynolds numbers turn out to be relatively small, $4/3$ is the β -value to be preferred in further calculations. Figure 15 illustrates the influence of the sink temperature.

As it has been remarked already, friction accelerates a subsonic flow. Consequently the length of the adiabatic section will influence the maximum heat throughput. This is illustrated by figure 16. The reduction of the throughput caused by friction, already substantial if there is no adiabatic section at all, strongly increases with increasing length of this section. It also has been remarked that friction values for wicked heat pipes might be up to three times the smooth pipe values. The impact of such a higher friction value is shown in figure 17.

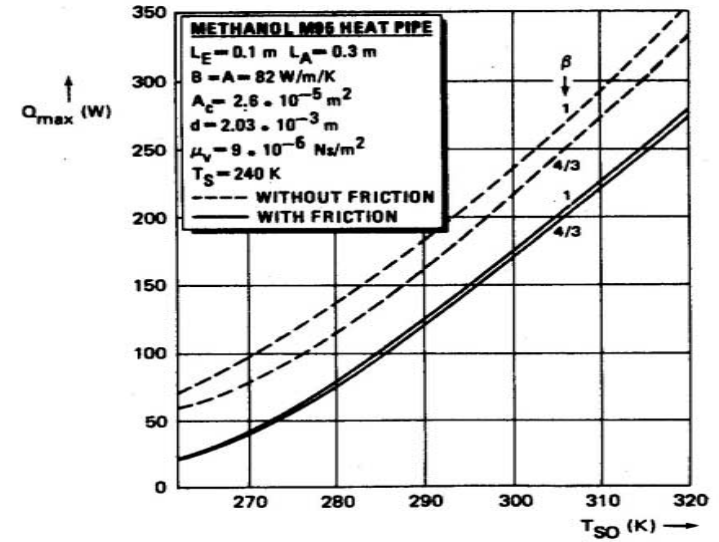


Figure 14. Maximum throughput versus source temperature for pure plug flow ($\beta=1$) and pure laminar flow $\beta=4/3$ (Ref. 8).

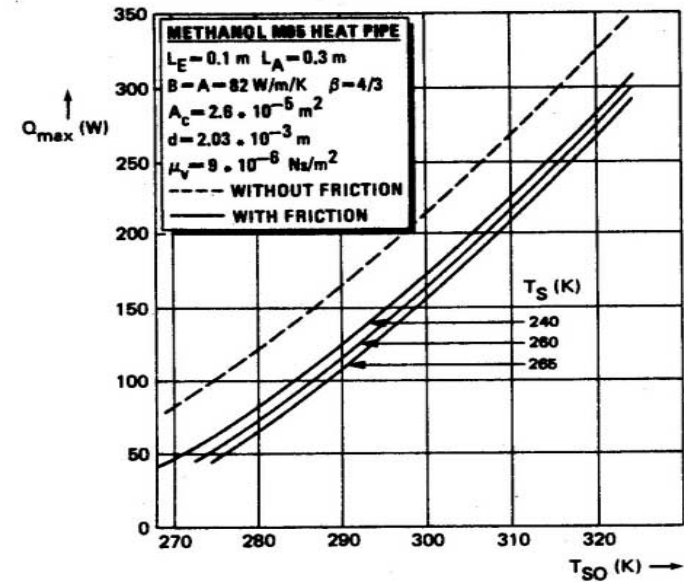


Figure 15. Maximum throughput versus source temperature, for various sink temperatures (Ref. 8).

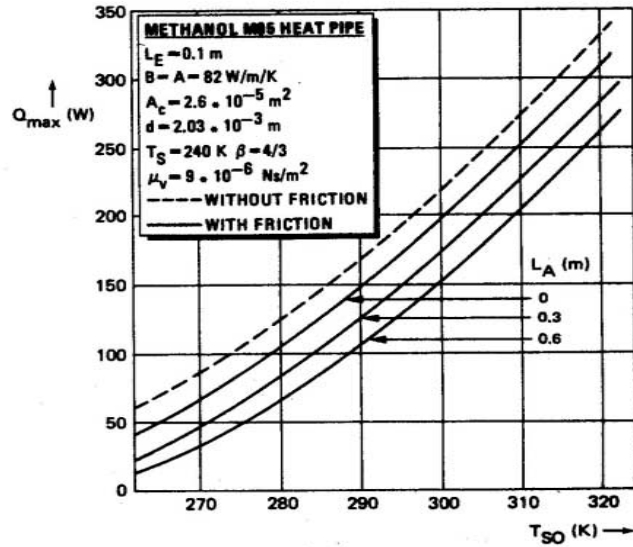


Figure 16. Maximum throughput versus source temperature for various adiabatic section lengths (Ref. 8).

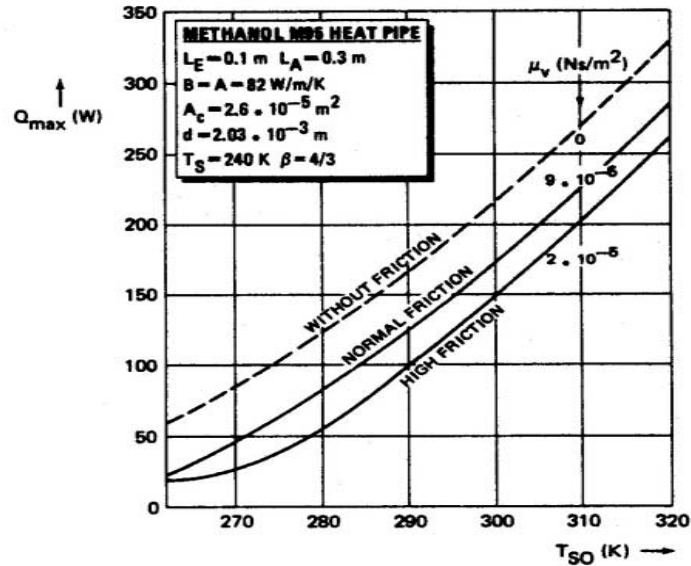


Figure 17. Maximum throughput versus source temperature for various values of the vapour viscosity (Ref. 8).

All calculations presented have been carried out using a value of 82 W/m.K for the equivalent radial conductances in the evaporator and the condenser. This value has been derived from heat pipe material properties, dimensions and a heat transfer coefficient of 4000 W/m²K, a value often used in the literature. However, especially in the evaporator, the heat transfer coefficients hence the equivalent radial conductance B can be much smaller. Figure 18 illustrates how important it is to know this conductance accurately.

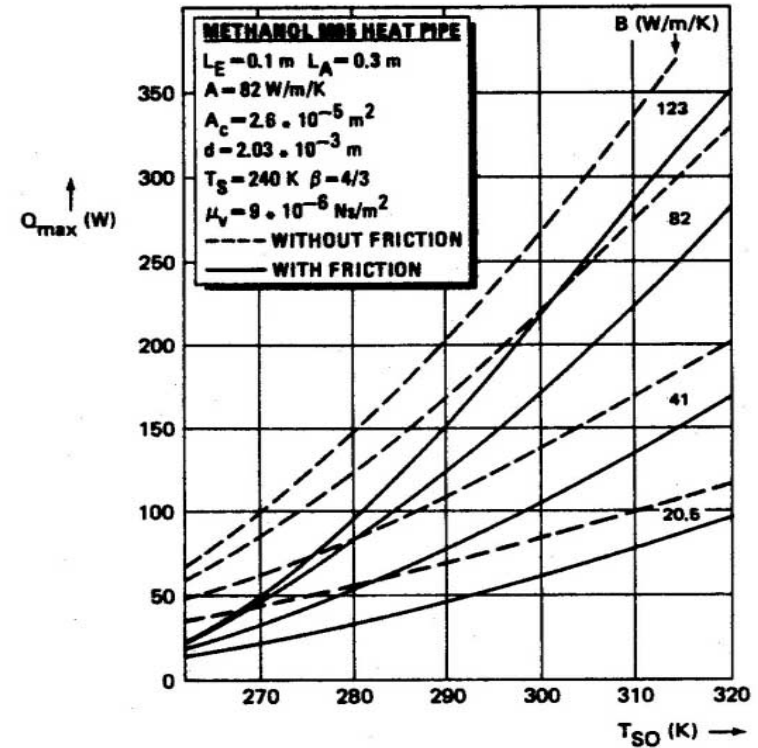


Figure 18. Maximum throughput versus source temperature, for various values of evaporator conductance (Ref. 8).

4.4. Control aspects

As it is remarked in the introduction, the control of the source temperature for varying thermal loading conditions is possible by actively adjusting the control gas pressure by influencing the reservoir quantities: size or temperature or molar gas content. Figure 11 presents the basic schematic of a feedback control system considered. Since the gas pressure p is a function of the throughput Q , the sink temperature T_S and the source temperature T_{SO} one can write

$$dp_g = (\partial p_g / \partial Q) dQ + (\partial p_g / \partial T_S) dT_S + (\partial p_g / \partial T_{SO}) dT_{SO} \quad (36)$$

The important transfer functions that can be identified, $(\partial p_g / \partial Q)$, $(\partial p_g / \partial T_S)$, and $(\partial p_g / \partial T_{SO})$, can be determined according to the equations (32) and (33) from figures like the upper part of figure 12 i.e. the relation between Q , x_r and T_r for various combinations of constant T_{SQ} and T_S and between T_S , x_r , T_r for combinations of constant T_S and Q .

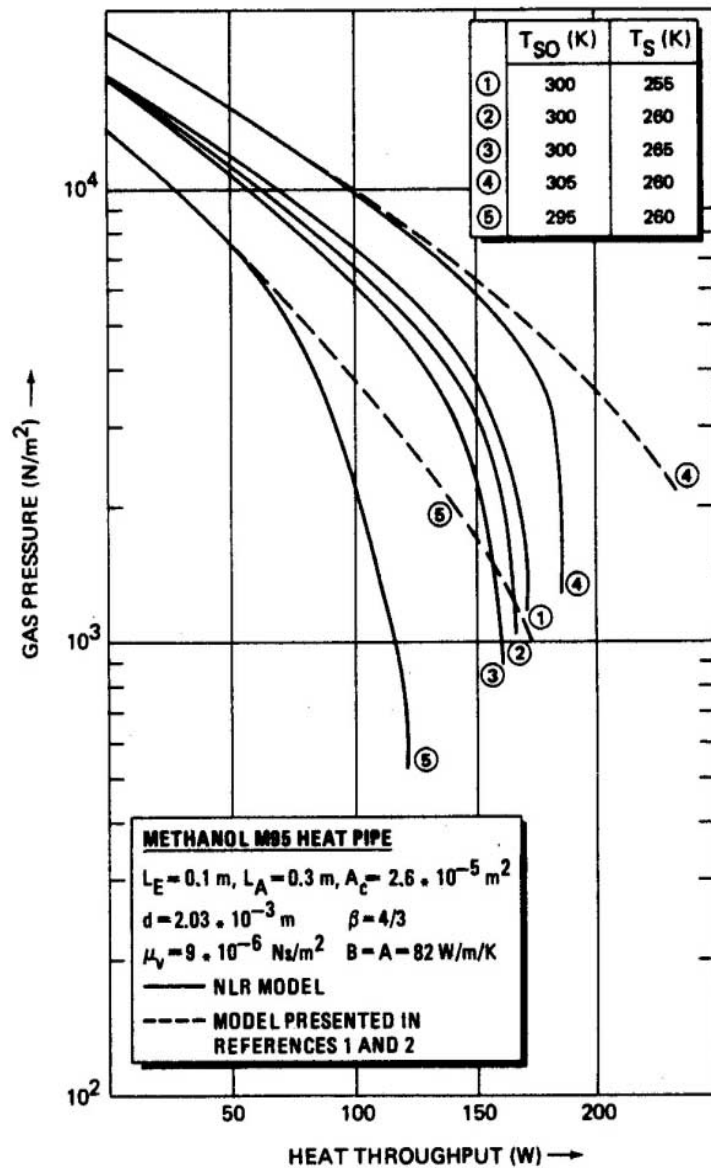


Figure 19. Gas pressure downstream of vapour-gas front versus power, for some source and sink temperatures (Ref. 8).

Figure 19 presents as an example, the relation between the gas pressure and the heat throughput for some source/sink temperature combinations. The derivative of the curves is the transfer function ($\partial p_g / \partial Q$). From this figure it can be concluded that the strong non-linearity for higher throughput values may lead to instabilities, considerably complicating the design of the control system, and may limit the operating range of the system.

The differences between the curves derived for the Edwards-Marcus model, which neglects friction and inertia, and the corresponding curves derived according to the NLR model, clearly illustrate the importance of the model for the determination of the parameters of the feedback control system.

Finally it can be remarked that for designing passive control systems, using a VCHP with fixed reservoir size, temperature and gas content, the curves are used to predict the magnitude of source temperature variations induced by variations in the thermal loading.

5. PTC IN THE VARIABLE CONDUCTANCE MODE OF A LOOP HEAT PIPE

A schematic of a Loop Heat Pipe (LHP) is shown in the right hand part of figure 20.

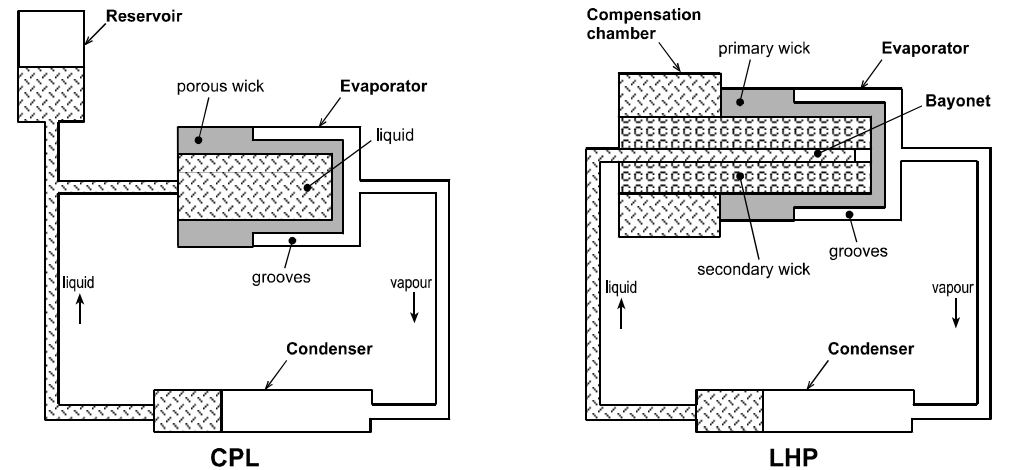


Figure 20. Capillary Pumped Loop (CPL) & Loop Heat Pipe (LHP), courtesy Jentung Ku, NASA GSFC.

Without going into detail one can easily see the variable conductance mode of the LHP, when looking at the typical performance graphs of the GLAS heat pipe, given in figure 21. The latter figure depicts the evaporator temperature as a function of the heat throughput for the two extreme cases, being a high superheat start-up and a low superheat start-up.

Both curves have a minimum, meaning that:

- Starting from the left side, an increasing of the heat input power will lead to a decreasing of the evaporator temperature till the minimum will be reached.
- A further increase of the input power will cause an increasing of the evaporator temperature, entering the LHP constant conductance mode, in which the evaporator temperature increases or decreases almost linear with input power.
- There is a variable conductance behaviour around the minima, since at a minimum dT_E/dQ changes sign.

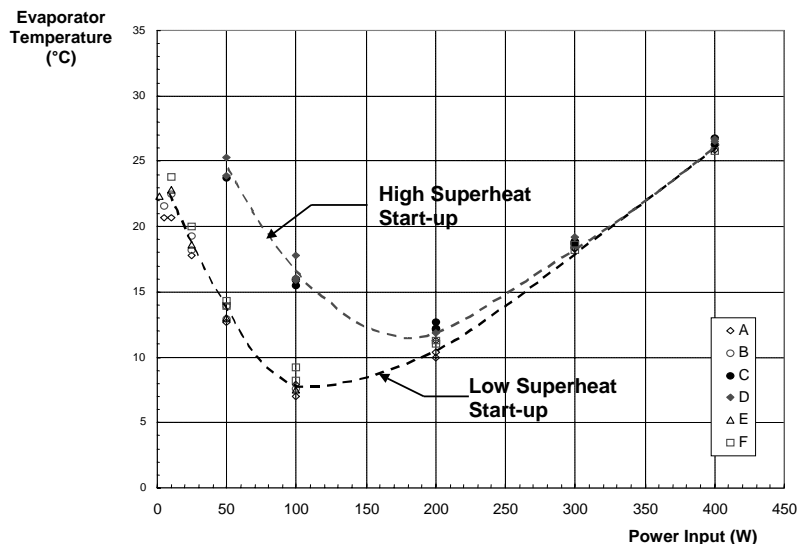


Figure 21. GLAS LHP performance: Evaporator temperature versus heat throughput (courtesy Jentung Ku, NASA GSFC).

6. IN CONCLUSION

Major issues of VCHP's have been discussed:

- The Edwards-Marcus model and its consequences for VCHP design for various applications.
- The refinement realised by the improved NLR VCHP thermal model.

Based on calculations with the NLR model, a M95 heat pipe with an adjustable external reservoir variable conductance VCHP has been designed, built and tested for the experimental verification of the NLR model for a gas-loaded VCHP (Ref. 20).

A parameter analysis for this heat pipe identified the different test conditions that will lead to the experimental confirmation of the predicted impact of inertia and friction on the heat pipe performance. The results obtained will constitute the basis for a further investigation of the active and passive control aspects of gas-loaded VCHP's.

In addition, the variable conductance mode in the Loop Heat Pipe has been briefly elucidated.

7. REFERENCES

1. Marcus, B.D., Theory and design of variable conductance heat pipes, NASA CR-2018, 1972.
2. Dunn, P.D. & Reay, D. A., Heat pipes, Pergamon Press, Oxford, 1976.
3. Chi, S.W., Heat pipe theory and practice, Hemisphere Publishing Corporation, Washington, 1976.
4. Edwards, D.K. & Marcus, B.D., Heat and mass transfer in the vicinity of the vapor-gas front in a gas-loaded heat pipe, J. of Heat Transfer Trans. ASME C 22, 1972, pp. 155-162.
5. Bienert, W. & Brennan, P., Study to evaluate the feasibility of a feedback controlled variable conductance heat pipe, NASA CR 73475, 1970.

6. Bienert, W. & Brennan, P., & Kirkpatrick, J.P., Feedback controlled variable conductance heat pipes, AIAA paper 71-421, AIAA 6th Thermophysics Conference, 1971.
7. Bienert, W. & Brennan, P., Transient performance of electrical feedback controlled variable conductance heat pipes, ASME paper 71-Av-27, 1971.
8. Delil, A.A.M., Limitations in variable conductance heat pipe performance and control predicted by the current steady state model developed at NLR, NLR-MP-1984-009, Proc. 5th International Heat Pipe Conference, Tsukuba, Japan, 1984, pp. 225-231.
9. Van der Vooren, J. & Delil, A.A.M. & Sanderse, A., Uniaxial model for a gas-loaded-variable conductance heat pipe, NLR-TR-80048, 1980.
10. Van der Vooren, J. & Sanderse, A., An improved flat front model for a gas-loaded variable conductance heat pipe, NLR-TR-80049, 1980.
11. Delil, A.A.M. & Van der Vooren, J., Uniaxial model for gas-loaded variable conductance heat pipe performance in the inertial flow regime, NLR-MP-81010 U, 1989, (Advances in heat pipe technology, Editor: Reay, D.A., Pergamon, Oxford).
12. Van de Wijngaart, R., Uniaxial model for the transient behaviour of the vapour/gas core in a gas-loaded variable conductance heat pipe, Thesis Delft Technological University, 1982.
13. Delil, A.A.M. & Daniëls, H.A.M., Uniaxial model for gas-loaded variable conductance heat pipe performance; The effects of vapour flow friction and inertia, NLR-MP-83058 (in ESA SP 200, Environmental and thermal systems for space vehicles), 1983.
14. Shapiro, A. H., Compressible fluid flow, Ronald Press Company, New York, 1953.
15. Ivanovskii, M.N. & Sorokin, V.P. & Yagodkin, I.V., The Physical Principles of Heat Pipes, Clarendon Press, Oxford, UK, 1982.
16. Delil, A A M, Theory and design of conventional heat pipes for space applications, NLR-TR-77001, 1977.
17. Scrabek, E.A. & Bienert, W.B., NASA Heat pipe design handbook, NASA CR 134264/265, 1972.
18. Levy, E.K., Effects of friction on the sonic velocity limit in sodium heat pipes, AIAA 6th Thermophysics Conference, Tullahoma, USA, 1971.
19. Levy, E.K. & Chou, S.F., The sonic limit in sodium heat pipes, J. of Heat Transfer Trans. ASME C, 6, 1973, pp. 218-223.
20. Van Buggenum, R.I.J. & Daniels, D.H.W., Development, manufacturing and testing of a gas-loaded variable conductance heat pipe, Proc. 6th Int. Heat Pipe Conference, Grenoble, France, 1987, pp. 330-337.